Transgenic Corneal Neurofluorescence in Mice: A New Model for In Vivo Investigation of Nerve Structure and Regeneration

Charles Q. Yu and Mark I. Rosenblatt

Purpose. To quantify the level of neuron-specific fluorescence in the corneas of transgenic mice expressing yellow fluorescent protein (YFP) driven by the *thy1* promoter and examine the viability of using *thy1*-YFP mice as a model for studying nerve regeneration in vivo.

Methods. The structure of corneal innervation in *thy1*-YFP mice visible with reporter gene fluorescence was compared with that visible with traditional immunofluorescence techniques. The percentage of corneal nerves with YFP fluorescence in wholemounted corneas and trigeminal neuron cultures was determined. Regeneration of fluorescent corneal neuronal processes after wounding was monitored in vivo.

Results. In the mouse cornea, neuron-specific immunostaining determined that nerves enter the stroma in several bundles that then extend throughout the entire cornea. These stromal nerve bundles form a subbasal plexus beneath the corneal epithelium. Fine nerves from this plexus travel superficially to the ocular surface. Neuron-specific expression of YFP allowed visualization of nearly all large nerve bundles of the stroma but only some of the many finer nerves of the subbasal plexus and surface. In the subbasal nerve plexus, 46% of total neuronal processes exhibited YFP neurofluorescence. In vitro, 22% of cultured trigeminal neurons exhibited YFP neurofluorescence. After corneal nerve transection, nerve processes distal to the site of injury degenerated, whereas those proximal to the site regenerated in a pattern different from original nerve architecture.

Conclusions. *Thy1*-YFP mice display neurofluorescence and provide a novel model for monitoring the patterning, injury, and growth of corneal nerves in vivo. (*Invest Ophthalmol Vis Sci.* 2007;48:1535–1542) DOI:10.1167/iovs.06-1192

The cornea is among the most densely innervated tissues of the human body, containing primarily sensory and some autonomic innervation.[1] In humans, corneal nerves mostly originate from the ophthalmic branch of the trigeminal nerve and enter the corneal stroma in a radial pattern from the limbus. They then form a subbasal plexus underneath the corneal epithelium, which extends thin nerve leashes that contain nociceptors present at the surface of the cornea.[2] Cell bodies of the sensory nerves of the cornea lie in the trigeminal ganglion.[3] Corneal nerves are of great importance due to their role in protecting the cornea from irritants as well as their trophic properties, which are necessary to maintain a healthy ocular surface. Disruption of the corneal nerves has been shown to impair corneal healing significantly.[4] In addition, many diseases such as herpetic viral infections and ophthalmic surgical procedures such as corneal transplantation, radial keratotomy, photorefractive keratectomy (PRK), and laser-assisted in situ keratomileusis (LASIK), cause corneal nerve disruption that can lead to conditions ranging from mild dry eye to severe neurotrophic keratitis with corneal melting.[5]

Many techniques have been used to examine corneal nerves. Most, such as electron microscopy or gold chloride, acetylcholinesterase, and immunohistochemical staining, cannot be performed on living organisms.[6] In vivo confocal microscopy has recently been used to photograph the subbasal plexus of humans and some animals, but is limited by the difficulty and quality of visualization as well as the availability of expensive equipment.[7–9]

Lines of C57BL/6 mice, which express the yellow–green fluorescent protein YFP driven by *thy1*, a promoter highly expressed in the nervous system, have been created.[10,11] These mice have fluorescence activity in many of their nerves and have been used to monitor sensory neuron degeneration in diabetic mice, observe tibial nerves, and investigate motor neuron disease in autoimmune encephalomyelitis.[12–14] In this study, we determined the levels of fluorescence gene expression in the corneal nerves of these transgenic *thy*1-YFP mice. We then used these mice as a means to investigate corneal nerve structure and study nerve regeneration after injury in vivo.

Materials and Methods

Animals

C57BL/6 mice of the *thy1*-YFP line 16 were purchased from Jackson Laboratories (Bar Harbor, ME). Heterozygous mice were bred to homozygosity. Homozygous and heterozygous mice were killed and photographed under identical conditions to evaluate relative YFP nerve fluorescence activity in their corneas. Mice homozygous for the *thy1*-YFP transgene were then used to establish a mouse colony for all further experimentation. For in vivo experiments, mice were anesthetized with an intraperitoneal injection of a combination of ketamine (20 mg/kg; Phoenix Scientific, St. Joseph, MO) and xylazine (6 mg/kg; Phoenix Scientific). For terminal experiments, mice were killed with a lethal dose of intraperitoneal pentobarbital (100 mg/kg; Abbott Laboratories, North Chicago, IL). All animals were male and approximately 5 weeks of age at time of experimentation. All experiments were conducted in accordance with the ARVO Statement for the Use of Animals in Ophthalmic and Vision Research.

Fluorescence Imaging

Animals and whole enucleated eyes were photographed with a fluorescence stereoscope (StereoLumar V.12) equipped with a digital camera (Axiocam MRm) and software (Axiovision 4.0). Slides of tissue sections and wholemounts were imaged with a motorized fluores-

From the Department of Ophthalmology and Vision Science, University of California Davis School of Medicine, Sacramento, California.

Supported by National Institutes of Health/National Eye Institute Grant K08EY015829 (MIR) and Vision Research Core Grant P30EY012576.

Submitted for publication October 5, 2006; revised November 21, 2006; accepted January 26, 2007.

Disclosure: **C.Q. Yu**, None; **M.I. Rosenblatt**, None

The publication costs of this article were defrayed in part by page charge payment. This article must therefore be marked "*advertisement*" in accordance with 18 U.S.C. §1734 solely to indicate this fact.

Corresponding author: Mark I. Rosenblatt, Dept. of Ophthalmology and Vision Science, University of California, Davis, 4860 Y Street, Suite 2400 Sacramento, CA 95817; mirosenblatt@ucdavis.edu.

cence microscope (AxioVert 200M, with Axiovision 4.0) equipped with a slider module (Axiocam MRm) for optical sectioning controlled by the system software (Axiovision 4.0; all are from Carl Zeiss Meditec GmbH, Oberkochen, Germany).

Trigeminal Ganglion and Cornea Cryosectioning and Immunohistochemistry

For examination of tissue sections, mice were killed, and eyes and trigeminal ganglia were excised, fixed in 4% paraformaldehyde for 40 minutes, embedded in optimal cutting temperature (OCT) media (Tissue-Tek, Torrance, CA) and snap frozen on dry ice. Sagittal and cross cryosections 8 μm thick were cut and mounted on glass slides (R 7200; Mercedes Medical, Sarasota, FL). These sections were permeabilized and blocked with a 1-hour incubation in 1% bovine serum albumin (BSA; Sigma-Aldrich, St. Louis, MO) in phosphate-buffered saline (PBS pH 7.0) and 0.1% Triton X-100 (Sigma-Aldrich). Sections were incubated with rabbit anti-mouse primary antibody specific for β III tubulin (Millipore, Billerica, MA), a marker highly expressed in all neurons,[15] at a dilution of 1:200 for 2 hours at room temperature. After three washes in PBS, sections were incubated in goat anti-rabbit secondary antibody conjugated to Texas Red (Jackson ImmunoResearch, West Grove, PA) at a dilution of 1:300 for 1 hour at room temperature. Sections were mounted in mounting medium containing DAPI (4′,6′-diamino-2-phenylindole; VectaShield; Vector Laboratories, Burlingame, CA), coverslipped, and imaged.

Trigeminal Neuron Culture and Immunocytochemistry

A procedure to culture trigeminal neurons from mice was adapted from a protocol for rats.[16] After death, mouse skull caps were removed. The brains were lifted to expose the trigeminal ganglia at the base of the skull cavity. The ganglia were cut at the anterior and posterior ends. The duras were incised along with any remaining connections. The ganglia were then removed, washed in calcium- and magnesium-free Hanks' solution (Invitrogen, Carlsbad, CA), diced into 5 to 10 pieces each, and incubated in papain 20 U/mL (Worthington Biochemical, Lakewood, NJ) for 20 minutes at 37°. After triturating and further incubation in 0.3% Dispase II (Roche, Basel, Switzerland) and 0.4% collagenase (Worthington Biochemical) for 20 minutes at 37°, the neuron cell bodies were concentrated by centrifugation through 30%/60% Percoll (Sigma-Aldrich) density gradients and plated on eight-well culture slides (Permanox; Nalge Nunc International, Rochester, NY) with Ham's F12 medium (Invitrogen) supplemented with 50 ng/mL 2.5 S nerve growth factor (NGF; Invitrogen, Carlsbad, CA) and 10% fetal bovine serum (Hyclone, Logan, UT). Cells from each pair of mouse trigeminal ganglia were plated in a single well.

After 48 hours' growth at 37° and 5% CO_2, media were removed from the wells and the cells were fixed in 2% paraformaldehyde for 20 minutes. The cells were then permeabilized with PBS containing 0.1% Triton X-100 and blocked with 1% BSA in PBS. Cells were incubated with anti-β III tubulin primary antibody at 1:2000 for 1 hour at room temperature, followed by detection using secondary antibody conjugated with Texas Red at 1:300 for an additional hour at room temperature. As a control, one well was not stained with primary antibody. Slides were coated with mounting medium with DAPI (VectaShield; Vector Laboratories), coverslipped, and imaged.

For each sample well, anti-β III tubulin staining was used to identify 10 fields of view containing cell bodies. These fields were photographed for Texas Red and YFP activity. For each control well, 10 random fields of view were photographed and processed due to lack of identifiable Texas Red activity. The total number of cell bodies visible with each filter in each well was recorded. The number of YFP-positive cells was divided by the number of Texas Red–positive cells to determine the percentage of neurons with YFP fluorescence.

Wholemount Examination of Cornea

Enucleated right eyes from *thy1*-YFP mice were fixed in 4% paraformaldehyde for 40 minutes at room temperature. Corneas were excised under a surgical scope and washed with PBS. Permeabilization and blocking was achieved with a 2-hour incubation in 1% BSA in PBS and 0.2% Triton X-100. Corneas were incubated with rabbit anti-mouse β III tubulin primary antibody at a dilution of 1:200 for 16 hours at 4°. After three washes in PBS, corneas were incubated in goat anti-rabbit secondary antibody conjugated to Texas Red at a dilution of 1:300 for 5 hours at 4°. After four relaxing radial incisions were made, the corneas were coverslipped with mounting medium containing DAPI (VectaShield; Vector Laboratories) and imaged.

Three fields of view at the level of the subbasal nerve plexus near the midpoint between the limbus and the apex of the cornea were photographed with both YFP and Texas Red filters. Nerve fibers were traced and the length calculated with commercial software (Adobe Illustrator; Adobe Systems, San Jose, CA) with an object-length function. The lengths of nerve processes found in the three fields of view were totaled and converted to micrometers of nerves per square millimeter. The density of nerve processes showing YFP activity was divided by the density of nerve processes labeled with Texas Red, to determine the percentage of YFP fluorescent nerve fibers.

Last, regions at the limbus and pericentral cornea were optically sectioned with the slider module (Apotome; Carl Zeiss Meditec, Inc.) to create a three-dimensional (3-D) reconstruction of nerve structure that was visible with YFP and Texas Red fluorescence.

Observation of Corneal Nerve Patterning In Situ

Thy1-YFP mice were killed, and eyes were observed for YFP activity using fluorescence stereomicroscopy. In one mouse, the left eye was marked for orientation and then enucleated. The eye was placed on the stage of the stereoscope and photographed for YFP activity from the superior, nasal, inferior, and temporal directions. The cornea was then dissected and imaged as a wholemount.

Evaluation of Corneal Nerve Regeneration In Vivo

An anesthetized *thy1*-YFP mouse was placed on the stage of a stereoscope (Carl Zeiss Meditec GmbH). The pupil was constricted with 2% pilocarpine (Alcon, Fort Worth, TX) and the cornea was anesthetized with 0.5% proparacaine (Bausch & Lomb, Tampa, FL). Under fluorescent and halogen stereoscopic observation, stromal nerve trunks were located, and a partial-thickness cut that severed a nerve bundle was made in the cornea with a scalpel blade. Photographs were taken before and after nerve sectioning. Similar fields of view of the same nerve were photographed 2, 6, and 13 days after injury. On day 24, the mouse was killed and the eye photographed for a final time.

Results

Effect of Transgene Copy Number on Corneal Neurofluorescence

Fluorescent nerve fibers were observed in the corneas of mice heterozygous and homozygous for the *thy1*-YFP transgene ($n = 3$). The level of identifiable fluorescence is notably higher in homozygous *thy1*-YFP mice (with twice the number of transgenes) both in terms of the total number of nerve fibers that can be detected and in the intensity of fluorescence in each fiber (Fig. 1).

Localization of Corneal Nerve Fibers by Transgenic Neuronal YFP Expression and Immunofluorescence

Cornea Cryosections. Cryosections of *thy1*-YFP mice corneas were stained for nerves and imaged. Neuron-specific anti-β III tubulin staining of cross sections showed large nerve bundles in the stroma, a dense network of small-diameter nerves beneath the corneal epithelium, and finer neuronal leashes extending superficially to the corneal surface (Fig. 2B). Transgenic neurofluorescence also revealed the larger nerve bundles of

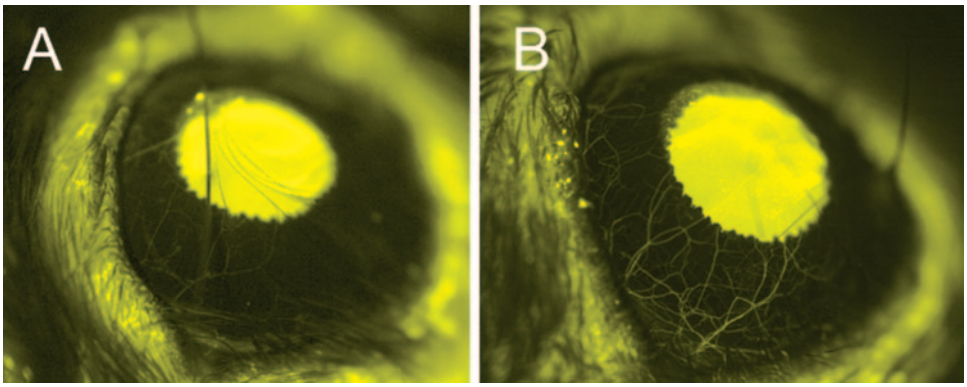

FIGURE 1. Effect of transgene copy number on corneal neurofluorescence. Right eyes of *thy1*-YFP transgenic mice were imaged with a fluorescence stereomicroscope. Both corneas were imaged using identical magnification, fluorescence intensity, and digital camera settings. The intensity and number of fluorescent nerves were lower in heterozygous *thy1*-YFP mice (**A**) compared with homozygous mice (**B**) possessing twice the number of transgene copies.

the stroma. However, less activity was observed in the subbasal plexus and in the epithelium. Most notably, very few transepithelial nerves were YFP positive in these sections (Fig. 2A).

Cornea Wholemounts. The right eyes of four *thy1*-YFP mice were enucleated, stained, wholemounted, and imaged. Anti-β III tubulin staining of wholemounted corneas and subsequent 3-D reconstruction (Apotome; Carl Zeiss Meditec, GmbH) showed nerve fibers entering at the limbus in bundles that then traveled and branched in the stroma. These nerves formed a subbasal plexus underneath the corneal epithelium and sent fibers up to the corneal surface. Nearly all large bundles of nerves of the stroma displayed YFP fluorescence, but many finer nerves of the subbasal plexus lacked observable YFP fluorescence (Fig. 3). Imaging of the subbasal plexus near the apex of the cornea demonstrated a spiral patterning of the nerve fibers at this layer which was observed in all eyes (Fig. 4).

Quantification of Transgenic Neurofluorescence

Trigeminal Neuron Culture. The trigeminal ganglion contains neuron cell bodies that provide sensory innervation to the face, including the cornea. In trigeminal ganglion cultures, fluorescent cell bodies with exuberant processes were observed after 24 hours growth in NGF supplemented media. Immunostaining confirmed that these were indeed neurons. Several cell morphologies were noted—in particular, some neuron cell bodies formed a dense mat of processes with marked branching, whereas other cell bodies sent out few processes with little branching (data not shown). The number of neurons seen in culture with transgenic YFP activity was compared with the total number of neurons present (those staining positive for β III tubulin; Fig. 5). Trigeminal cultures of mice ($n = 4$) showed 21.9% $\pm$ 2.6% (SEM) of neuron bodies exhibiting visible neurofluorescence (Table 1). Examination of trigeminal cross-sections from *thy1*-YFP mice demonstrated a similar ratio of YFP-positive to anti-β III tubulin–positive neuronal cell bodies (Fig. 6).

Subbasal Plexus Activity. The right corneas of the same mice were excised, wholemounted, and imaged. Neuronal processes of the subbasal plexus were photographed. The length of nerve processes in the subbasal plexus that had YFP activity was compared to the total length of anti-β III tubulin–positive nerve processes in the plexus. Of the subbasal nerves in the plexus, 46.1% $\pm$ 2.1% (SEM) were YFP positive (Fig. 7; Table 1).

Application of Neurofluorescence

Pattern of YFP Positive Corneal Nerves. YFP activity of mouse corneal nerves was used to observe the innervation in intact eyes of four recently killed mice. Nerves were seen to enter the cornea at the limbus in three regions in large bundles that then branched extensively. In one mouse, the left eye was enucleated and photographed from the superior, nasal, inferior, and temporal directions (Fig. 8). This confirmed that nerves entered the stroma at the limbus in approximately three bundles at the 3, 6, and 9 o'clock hours. These bundles then branched into finer nerve processes that cover the entire cornea.

Nerve Sectioning and Regeneration. Under simultaneous fluorescent and halogen illumination, a partial thickness incision in the cornea of an anesthetized *thy1*-YFP mouse was made that severed a large YFP+ nerve bundle. Two days after this injury, the

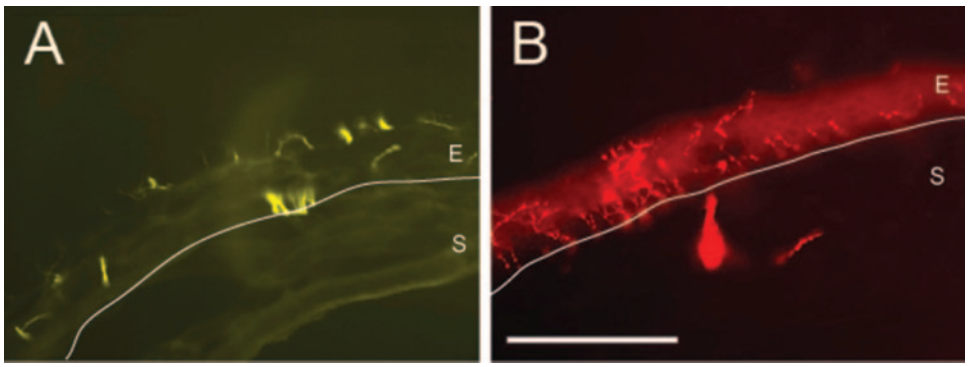

FIGURE 2. Neuronal localization in *thy1*-YFP mouse cornea. The distribution of neuronal processes was localized in 8-μm-thick cryosections of corneas (**A**, **B**) from *thy1*-YFP mice. The number of nerves visualized by transgenic corneal neurofluorescence (**A**) was fewer than were identifiable by anti-β III tubulin (a pan-neuronal marker) immunofluorescence (**B**), although in both imaging techniques, a subbasal plexus of corneal nerves with leashes of nerve endings extending into the epithelium was detectable. (**A**, **B**) *White line*: junction between the corneal stroma (S) and epithelium (E). Scale bar, 100 μm.

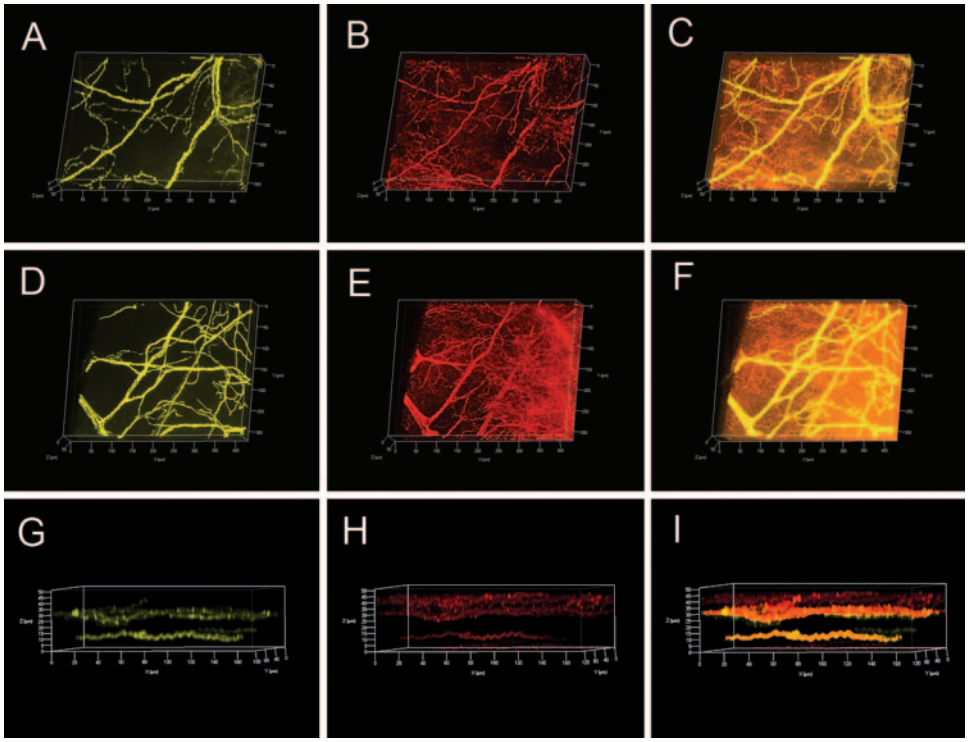

FIGURE 3. Localization of fluorescent nerves in *thy1*-YFP mouse cornea wholemounts. Corneal nerves were localized in wholemounts from *thy1*-YFP mice via transgenic corneal neurofluorescence (**A**, **D**, **G**) and immunostaining for anti-β III tubulin (**B**, **E**, **H**). Separate imaging was performed at the corneal periphery (**A–C**) and pericentrally (**D–I**) using a structured grid illumination technique to obtain optical sections for subsequent 3-D reconstructions (Apotome; Carl Zeiss Meditec GmbH). Stromal nerve bundles and finer nerves of the subbasal plexus were seen by transgenic corneal neurofluorescence (**A**, **D**) and anti-β III tubulin immunofluorescence (**B**, **E**). Colocalization (**C**, **F**) indicates that whereas all the nerve bundles in the stroma were well visualized using both modalities, only a fraction of the subbasal nerves were visualized via transgenic neurofluorescence. Cross-sections obtained by 3-D reconstruction (**G–I**) localized stromal bundles by YFP detection as well as immunodetection. Transgenic neurofluorescence labeled many nerves of the subbasal plexus, but very few of the superficially directed nerve fibers (**G**). In contrast, a dense subbasal plexus as well as numerous fibers directed to the corneal surface were revealed by anti-β III tubulin immunostaining (**H**). Colocalization (**I**) demonstrated that the more superficial fibers were less likely to display transgenic neurofluorescence.

previously detectable neuronal processes distal to the cut were no longer detectable. Many small nerve processes that sprouted from the proximal end of the severed nerve bundle were observed. These small processes had a nonspecific orientation and did not extend past the original site of injury. Six and 13 days after surgery, directed nerve regeneration could be seen and several neuronal projections emanating from the severed nerve bundle had regenerated past the cut. At least one branch had assumed a novel branching morphology, indicating that the regenerating nerves did not follow the same course as the original nerves. At day 24 after injury, additional finer branches extended from the regenerating nerve bundle (Fig. 9). The new pattern of innervation did not resemble the initial pattern, and although there was an array of new neuronal processes, they did not extend as far as the original nerve.

DISCUSSION

We were able to examine the organization of corneal innervation in the mouse eye using conventional immunofluorescence

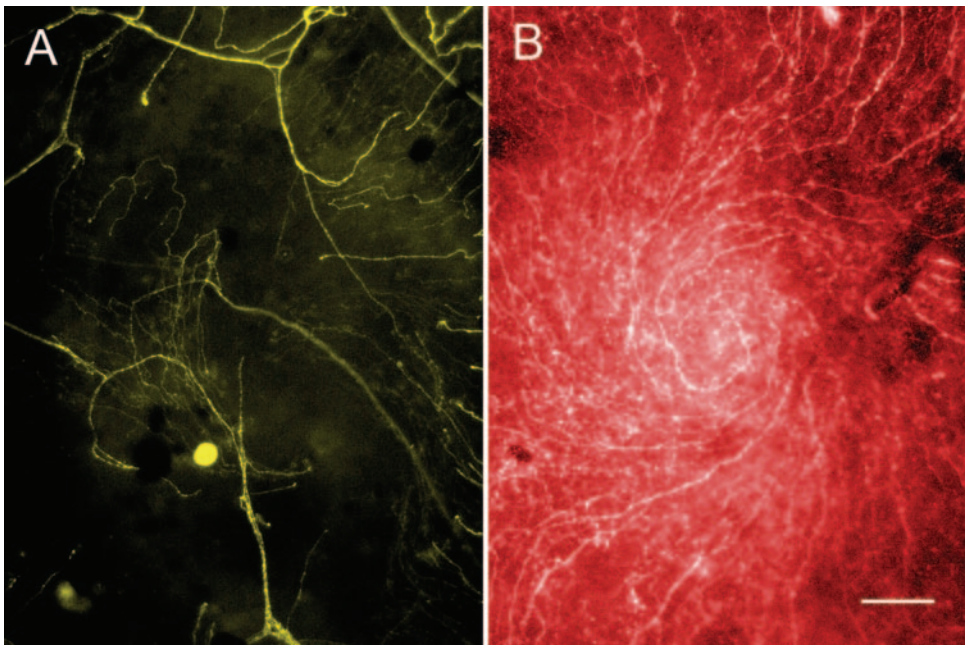

FIGURE 4. Spiral patterning of the mouse cornea subbasal nerve plexus. The innervation of the cornea near the apex in wholemounts from *thy1*-YFP mice was imaged using transgenic neurofluorescence (**A**) and anti-β III tubulin immunofluorescence (**B**). A spiral pattern of nerve termination at the central cornea was observed using both imaging modalities. Scale bar, 100 μm.

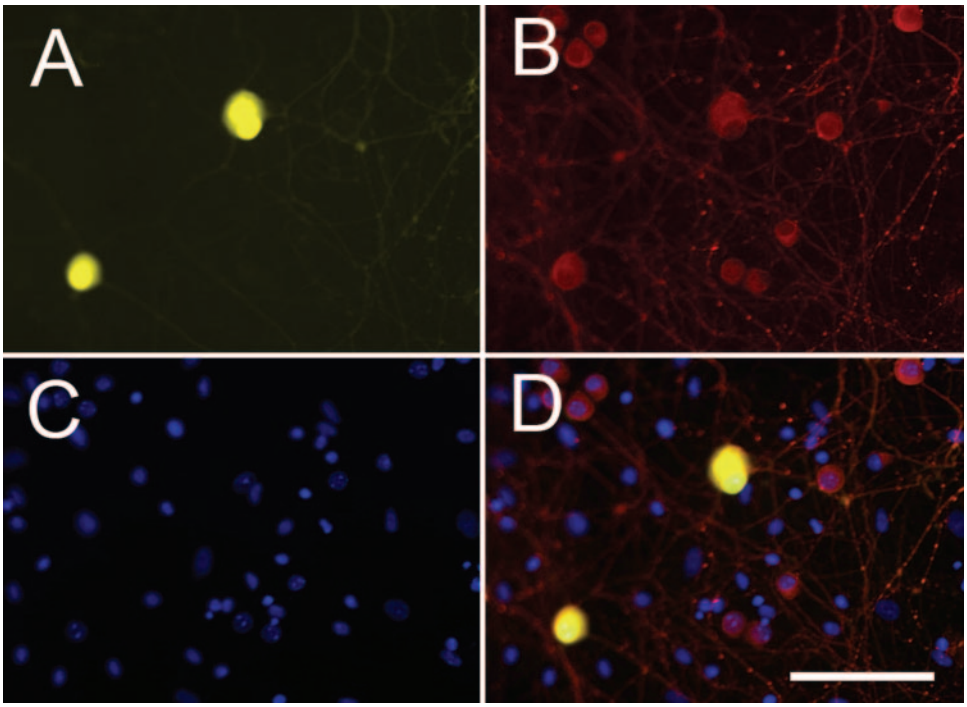

FIGURE 5. Quantification of transgenic neurofluorescence in cultured *thy1*-YFP mouse trigeminal neurons. Two days after plating, primary trigeminal cultures were immunostained with anti-β III tubulin to label neurons and were mounted in medium containing DAPI. A subpopulation of anti-β III tubulin–positive neurons (**B**) was found to be labeled by YFP (**A**). DAPI staining showed all cell nuclei (**C**). (**D**) Merger of images (**A–C**). Scale bar, 100 μm.

as well as a new in vivo model that utilizes a tissue-specific fluorescent reporter localized to neuronal subsets. Our data indicate that nerves enter the stroma of the murine cornea as three to four bundles at the periphery, which then branch as they move toward the center. Stromal branches give rise to a dense subbasal nerve plexus, which in turn sends nerve endings anteriorly to the ocular surface. The overall structure of corneal innervation of the mouse parallels that seen in other mammalian species.[17] However, given the increasing importance of mouse models of corneal disease, our results provide greater details on the murine corneal innervation that shed light on the alterations of neuronal patterning in these models.

There is conflicting information regarding the structure of the subbasal nerve plexus near the apex of the cornea. In humans, Muller et al.[17] indicated a superior to inferior architecture, whereas Patel et al.[7] observed a whorllike pattern. Similar to the observations of Patel et al., our mice showed a whorling subbasal nerve pattern, although the spiraling of nerves in the mouse cornea is more pronounced. This spiral pattern is similar to the known migration pattern of corneal epithelial cells as they move from the limbus to the central cornea.[18] Given the apposition of the subbasal plexus nerves with the corneal basal epithelium, it is possible that either epithelial migration patterns the corneal nerves or that the corneal innervation governs the path of migrating epithelium. Alternatively, other elements within the cornea could be simultaneously imprinting a pattern on both nerves and epithelium.

In addition, our immunostaining showed that mouse corneas have a high density of nerves in their subbasal plexus, with approximately 94,187 μm of nerves per square millimeter. Previous studies indicated a density of 20,000 to 25,000 μm/mm^2 for the human corneal subbasal plexus.[7] The reasons

TABLE 1. Transgenic Neurofluorescence of Trigeminal Cultures and Cornea Wholemounts from *Thy1*-YFP Mice

	Trigeminal Culture			Wholemount Subbasal Plexus Nerve Density		
Mouse	YFP+ (#)	Anti-β III Tubulin+ (#)	Transgenic Neurofluorescence	YFP+ Nerves (μm/mm^2)	Anti-β III Tubulin+ (μm/mm^2)	Transgenic Neurofluorescence
1	14	61	23.0%	36,125	88,026	41.0%
2	11	38	28.9%	50,183	101,740	49.3%
3	7	40	17.5%	50,526	101,225	49.9%
4	13	72	18.1%	37,981	85,758	44.3%
Control	2	0	n/a	47,433	0	n/a
Mean of 1–4 (±SEM)	11.25	52.75	21.9% ± 2.6%	43,704 ± 3,859	94,187 ± 4,239	46.1% ± 2.1%

Trigeminal ganglion neurons from *thy1*-YFP mice ($n = 4$) were cultured, stained for β III tubulin, and imaged for the colocalization of transgenic YFP neurofluorescence as in Figure 5. Ten neuron-containing fields per well were identified by the presence of anti-β III tubulin–staining and the total number of YFP and anti-β III tubulin–positive cells in these fields was determined. Ten random fields of view were used for control wells containing no primary antibody and thus no anti-β III tubulin staining. Corresponding right corneas of subject mice were dissected, stained with anti-β III tubulin, and imaged. Three random fields of view at the level of the subbasal plexus were photographed and the lengths of YFP-positive and anti-β III tubulin–positive neuronal processes were quantified as in Figure 7. Control wholemount corneas were not stained with primary antibody.

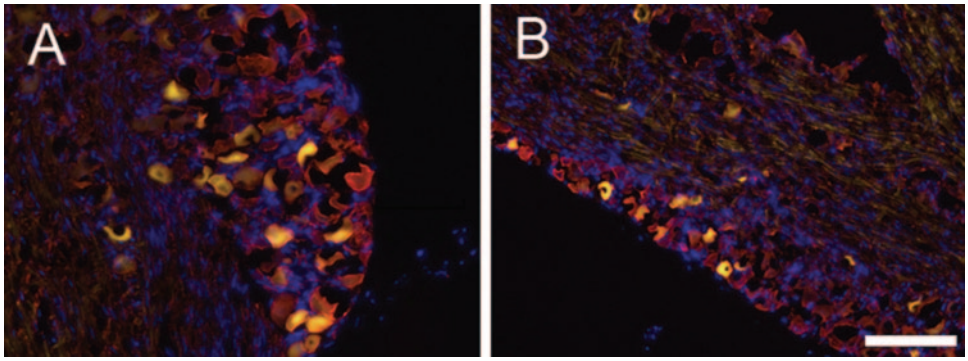

FIGURE 6. Transgenic fluorescence in the trigeminal ganglion. Transgenic YFP neurofluorescence (*yellow*), anti-β III tubulin immunofluorescence (*red*), and DAPI (*blue*) were colocalized in cross-sections (**A**) and sagittal sections (**B**) of *thy1*-YFP mouse trigeminal ganglions. Only a subset of the anti-β III tubulin–positive cells bodies demonstrated transgenic neurofluorescence. Scale bar, 100 μm.

for this observed difference are not known, but a higher density may be evolutionarily favored by either anatomic or functional requirements specific to the mouse.

The *thy1*-YFP transgenic line appears to be a bona fide model for studying corneal nerves. All large nerve bundles entering the cornea can be detected in vivo by virtue of transgenic YFP neurofluorescence. We examined the corneal subbasal nerve plexus of these transgenic mice and found that 46.1% ± 2.1% (SEM) of nerve processes was neurofluorescent. Similar examination of trigeminal neuron primary cultures found that 21.9% ± 2.6% (SEM) of cell bodies was fluorescent. Characterization by other investigations of more than 20 separate lines obtained from transgenic reporter constructs made with the *thy1* promoter and various fluorescent reporter genes demonstrated a high variability in neuronal expression both in terms of the subset of neurons labeled and in the percentage of each subset labeled.[14] Therefore, it is not surprising that not all corneal neurons were detectable by YFP imaging in our mice or that the trigeminal ganglion, which innervates many different tissues, does not have the same level of neurofluorescence. Indeed, only 1% to 5% of neuronal cell bodies in the trigeminal ganglion send processes to the cornea.[19,20] This observation indicates that the subset of labeled nerves is not geographically restricted to only a given region of the cornea. Also, because nearly half of all nerves show YFP activity in wholemounts, it is unlikely that only a single type of sensory nerve expresses YFP. A percentage of all sensory nerve types likely has YFP activity. This conclusion is bolstered by the finding that multiple neuronal morphologies displayed transgenic neurofluorescence in cultures of trigeminal neurons. The fact that nerve bundles in the stroma were nearly all observable using transgenic fluorescence is consistent with our findings because each bundle contained many nerves, and if a percentage of these nerves fluoresced, then the entire bundle would be visible. Last, it is important to note the low level of variance (<3% SEM) in levels of corneal neurofluorescence exhibited by different *thy1*-YFP mice.

Our observations indicate that distal neuron processes lose their fluorescent activity soon after they are severed, which is consistent with neuronal degeneration observed after injury in other systems.[21] New neuronal growth demonstrates fluorescent activity during regeneration, allowing for convenient tracing. Because the proximal end of the cut nerve had a number of sprouts (albeit poorly oriented) 2 days after initial surgery, it is likely that corneal nerves begin to regenerate quite soon after they have been damaged. Our data indicate that corneal nerves do not regenerate along their original path, but instead in a novel pattern after sectioning. This suggests that there are no preset pathways in which nerves travel when reinnervating the cornea.

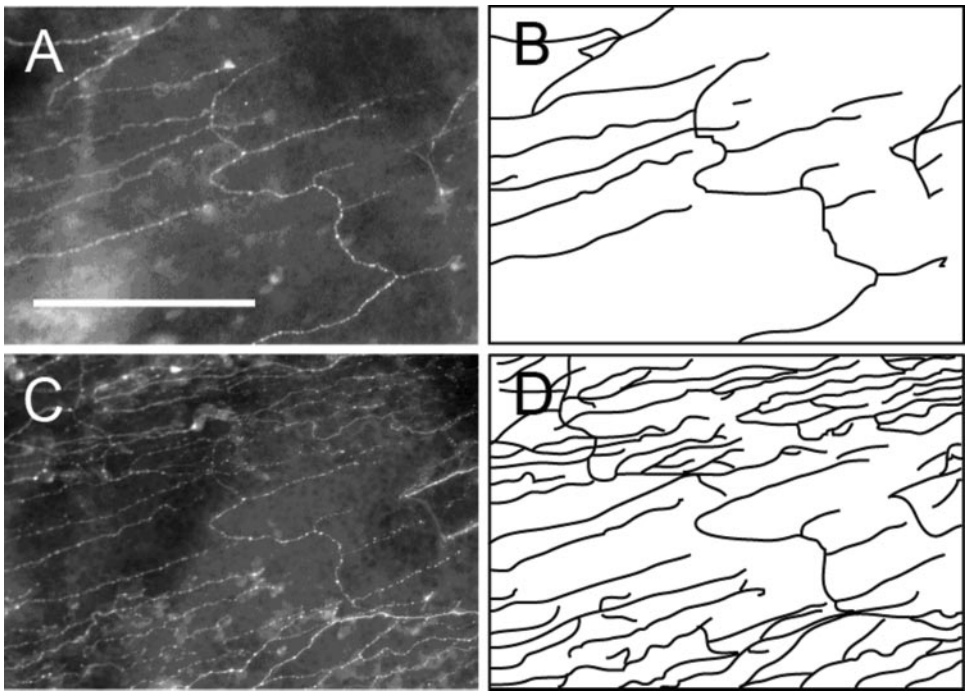

FIGURE 7. Quantification of transgenic neurofluorescence in the subbasal plexus of *thy1*-YFP mouse corneas. Corneal wholemounts from *thy1*-YFP mice were immunostained with anti-β III tubulin and imaged with the subbasal plexus in focus. A single field was imaged for YFP labeled nerves (**A**) and anti-β III tubulin positive nerves (**C**). Nerves were traced, and the total length calculated. In these images, YFP-positive neuronal processes measured 2585 μm (**B**) and anti-β III tubulin–positive processes measured 6645 μm (**D**). Scale bar, 200 μm.

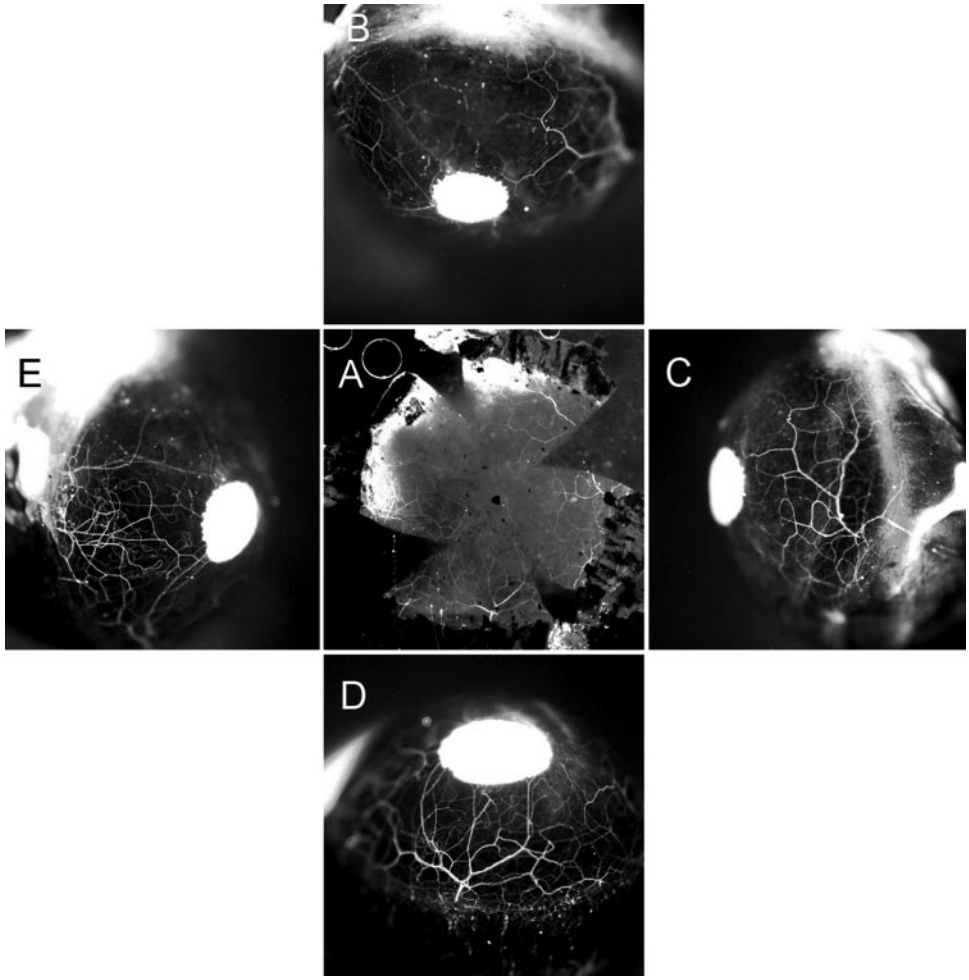

FIGURE 8. Pattern of innervation of the mouse cornea. The left eye of a *thy1*-YFP mouse was enucleated and the transgenic YFP neurofluorescence of the superior (**B**), inferior (**D**), nasal (**C**), and temporal (**E**) intact globe and the wholemount preparation (**A**) was visualized with a stereofluorescence microscope. YFP activity showed nerves entering the cornea in the nasal, temporal, and inferior regions.

The *thy1*-YFP model provides an important new tool for examining the regeneration of neurons in vivo. Previous investigators looked at nerve regeneration in several corneal injury models including full- and partial-thickness incisions, cryodestruction, excimer laser ablation, and epithelial debridement.[22,23] However, each of these techniques was limited by

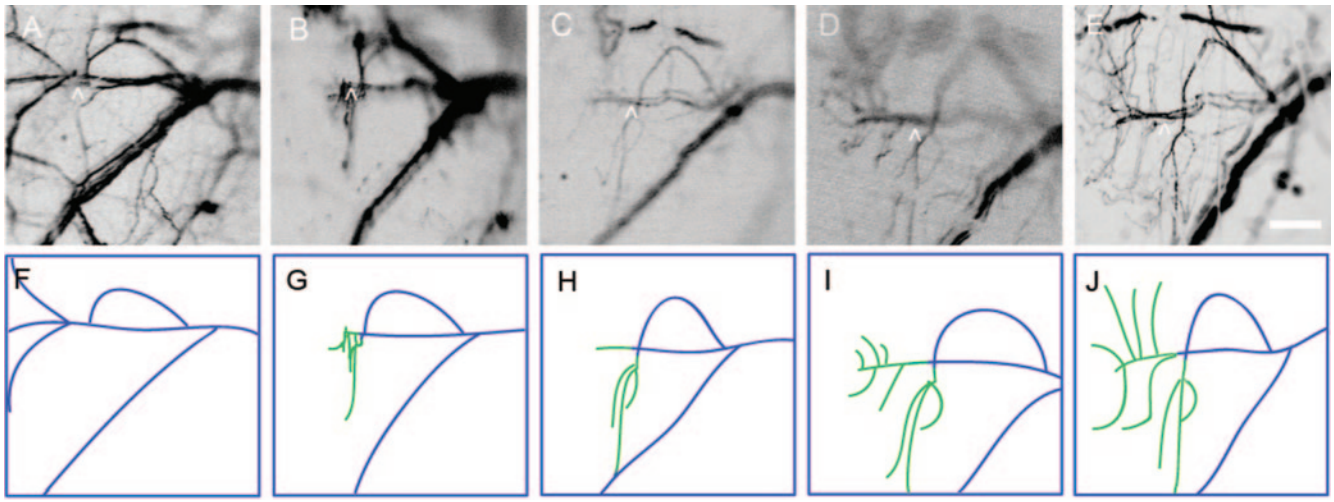

FIGURE 9. In vivo observation of nerve regeneration in the *thy1*-YFP mouse cornea. A *thy1*-YFP mouse was anesthetized and secured on the stage of a stereofluorescence microscope. Using fluorescence illumination, a partial-thickness incision was created in the cornea to sever a stromal corneal nerve. (**A–E**) Site of cut. The injured nerve of the same animal was imaged at days 0 (**A**), 2 (**B**), 6 (**C**), and 13 (**D**) and after death at day 24 (**E**). Below each image (**F–J**) is a corresponding drawing approximately depicting the original (*blue*) and regenerating (*green*) course of the injured corneal nerve. After injury (**A**, **F**), the fluorescence signal from the distal axons rapidly disappeared (**B**, **G**) and was not detectable at day 2. New axonal sprouting was observed on day 2 (**B**, **G**), and axonal growth continued in a pattern different from the original innervation (**A**, **F**) through day 24 (**C–E**, **H–J**). Scale bar, 100 μm.

the inability to follow the regeneration of specific neurons in a single animal. Conclusions were based on grouped data from postmortem analysis of groups of animals killed at serial time points. In contrast, we injured specific nerves with a partial-thickness incision and then observed these nerves as they regenerated in vivo without the need to kill animals at multiple time points.

Thy1-YFP mice display neurofluorescence in their corneas and allow the observation of corneal neuronal growth in living animals. These mice are useful for the examination of corneal innervation after injury and provide a novel and effective model for studying neuron regeneration in vivo.

References

1. Marfurt CF, Ellis LC. Immunohistochemical localization of tyrosine hydroxylase in corneal nerves. *J Comp Neurol*. 1993;336:517–531.
2. Muller LJ, Vrensen GF, Pels L, Cardozo BN, Willekens B. Architecture of human corneal nerves. *Invest Ophthalmol Vis Sci*. 1997; 38:985–994.
3. Lazarov NE. Comparative analysis of the chemical neuroanatomy of the mammalian trigeminal ganglion and mesencephalic trigeminal nucleus. *Prog Neurobiol*. 2002;66:19–59.
4. Murphy CJ, Marfurt CF, McDermott A, et al. Spontaneous chronic corneal epithelial defects (SCCED) in dogs: clinical features, innervation, and effect of topical SP, with or without IGF-1. *Invest Ophthalmol Vis Sci*. 2001;42:2252–2261.
5. Wilson SE, Ambrosio R. Laser in situ keratomileusis-induced neurotrophic epitheliopathy. *Am J Ophthalmol*. 2001;132:405–406.
6. Esquenazi S, Bazan HE, Bui V, He J, Kim DB, Bazan NG. Topical combination of NGF and DHA increases rabbit corneal nerve regeneration after photorefractive keratectomy. *Invest Ophthalmol Vis Sci*. 2005;46:3121–3127.
7. Patel DV, Sherwin T, McGhee CN. Laser scanning in vivo confocal microscopy of the normal human corneoscleral limbus. *Invest Ophthalmol Vis Sci*. 2006;47:2823–2827.
8. Labbe A, Liang H, Martin C, Brignole-Baudouin F, Warnet JM, Baudouin C. Comparative anatomy of laboratory animal corneas with a new-generation high-resolution in vivo confocal microscope. *Curr Eye Res*. 2006;31:501–509.
9. Tervo T, Moilanen J. In vivo confocal microscopy for evaluation of wound healing following corneal refractive surgery. *Prog Retin Eye Res*. 2003;22:339–358.
10. Feng G, Mellor RH, Bernstein M, et al. Imaging neuronal subsets in transgenic mice expressing multiple spectral variants of GFP. *Neuron*. 2000;28:41–51.
11. Gordon JW, Chesa PG, Nishimura H, et al. Regulation of Thy-1 gene expression in transgenic mice. *Cell*. 1987;50:445–452.
12. Myckatyn TM, Mackinnon SE, Hunter DA, Brakefield D, Parsadanian A. A novel model for the study of peripheral-nerve regeneration following common nerve injury paradigms. *J Reconstr Microsurg*. 2004;20:533–544.
13. Bannerman PG, Hahn A, Ramirez S, et al. Motor neuron pathology in experimental autoimmune encephalomyelitis: studies in THY1-YFP transgenic mice. *Brain*. 2005;128:1877–1886.
14. Chen YS, Chung SS, Chung SK. Noninvasive monitoring of diabetes-induced cutaneous nerve fiber loss and hypoalgesia in thy1-YFP transgenic mice. *Diabetes*. 2005;54:3112–3118.
15. Katsetos CD, Legido A, Perentes E, Mork SJ. Class III beta-tubulin isotype: a key cytoskeletal protein at the crossroads of developmental neurobiology and tumor neuropathology. *J Child Neurol.* 2003;18:851–866; discussion 867.
16. Eckert SP, Taddese A, McCleskey EW. Isolation and culture of rat sensory neurons having distinct sensory modalities. *J Neurosci Methods*. 1997;77:183–190.
17. Muller LJ, Marfurt CF, Kruse F, Tervo TM. Corneal nerves: structure, contents and function. *Exp Eye Res*. 2003;76:521–542.
18. Collinson JM, Chanas SA, Hill RE, West JD. Corneal development, limbal stem cell function, and corneal epithelial cell migration in the Pax6$^{+/-}$ mouse. *Invest Ophthalmol Vis Sci*. 2004;45:1101–1108.
19. Marfurt CF, Kingsley RE, Echtenkamp SE. Sensory and sympathetic innervation of the mammalian cornea: a retrograde tracing study. *Invest Ophthalmol Vis Sci*. 1989;30:461–472.
20. LaVail JH, Johnson WE, Spencer LC. Immunohistochemical identification of trigeminal ganglion neurons that innervate the mouse cornea: relevance to intercellular spread of herpes simplex virus. *J Comp Neurol*. 1993;327:133–140.
21. Coleman M. Axon degeneration mechanisms: commonality amid diversity. *Nat Rev Neurosci*. 2005;6:889–898.
22. Trabucchi G, Brancato R, Verdi M, Carones F, Sala C. Corneal nerve damage and regeneration after excimer laser photokeratectomy in rabbit eyes. *Invest Ophthalmol Vis Sci*. 1994;35:229–235.
23. Rozsa AJ, Guss RB, Beuerman RW. Neural remodeling following experimental surgery of the rabbit cornea. *Invest Ophthalmol Vis Sci*. 1983;24:1033–1051.